

East Tennessee State University

Digital Commons @ East Tennessee State University

ETSU Faculty Works

Faculty Works

11-1-2007

Neon Abundances from a Spitzer/IRS Survey of Wolf-Rayet Stars.

Richard Ignace

East Tennessee State University

J. Cassinelli

University of Wisconsin

G. Tracy

University of Wisconsin

E. Churchwell

University of Wisconsin

H. J. Lamers

Utrecht University

Follow this and additional works at: <https://dc.etsu.edu/etsu-works>



Part of the [Stars, Interstellar Medium and the Galaxy Commons](#)

Citation Information

Ignace, Richard; Cassinelli, J.; Tracy, G.; Churchwell, E.; and Lamers, H. J.. 2007. Neon Abundances from a Spitzer/IRS Survey of Wolf-Rayet Stars.. *The Astrophysical Journal*. Vol.669 ISSN: 2041-8205

This Article is brought to you for free and open access by the Faculty Works at Digital Commons @ East Tennessee State University. It has been accepted for inclusion in ETSU Faculty Works by an authorized administrator of Digital Commons @ East Tennessee State University. For more information, please contact digilib@etsu.edu.

Neon Abundances from a Spitzer/IRS Survey of Wolf-Rayet Stars.

NEON ABUNDANCES FROM A *SPITZER*/IRS SURVEY OF WOLF-RAYET STARS

R. IGNACE

Department of Physics, Astronomy, and Geology, East Tennessee State University, Johnson City, TN 37614; ignace@etsu.edu

J. P. CASSINELLI, G. TRACY, AND E. CHURCHWELL

Department of Astronomy, University of Wisconsin, 475 North Charter Street, Madison, WI 53706; joecass@astro.wisc.edu, gatracy@wisc.edu, ebc@astro.wisc.edu

AND

H. J. G. L. M. LAMERS

Astronomical Institute, Utrecht University, Princetonplein 5, 3584 CC Utrecht, The Netherlands; H.J.G.L.M.Lamers@astro.uu.nl

Received 2007 April 27; accepted 2007 July 19

ABSTRACT

We report on neon abundances derived from *Spitzer* high resolution spectral data of eight Wolf-Rayet (WR) stars using the forbidden line of [Ne III] $15.56\ \mu\text{m}$. Our targets include four WN stars of subtypes 4–7, and four WC stars of subtypes 4–7. We derive ion fraction abundances γ of Ne^{2+} for the winds of each star. The ion fraction abundance is a product of the ionization fraction Q_i in stage i and the abundance by number \mathcal{A}_E of element E relative to all nuclei. Values generally consistent with solar are obtained for the WN stars, and values in excess of solar are obtained for the WC stars.

Subject headings: stars: abundances — stars: mass loss — stars: winds, outflows — stars: Wolf-Rayet

1. INTRODUCTION

Wolf-Rayet (WR) stars continue to attract the attention of many researchers because they are evolved massive stars that are useful for testing stellar evolutionary models and because they have extremely massive winds (Lamers et al. 1991; Meynet & Maeder 2003). We report on infrared observations of [Ne III] $15.56\ \mu\text{m}$ for eight WR stars, each of a different spectral subtype (see Table 1), obtained with the *Spitzer* Infrared Spectrograph (IRS) using the Short-High (SH) mode in the 10–20 μm band. Details about the *Spitzer* telescope and particularly the IRS instrument can be found in Houck et al. (2004). Our program targeted four nitrogen-rich WN stars, and four carbon-rich WC stars. Subtypes WN4–WN7 and WC4–WC7 were selected to avoid complications associated with the late subtypes, namely that the WC8 and WC9 types often show dust production (e.g., van der Hucht et al. 1981; Williams 1997; Monnier et al. 2007), and the WN8 types are associated with significant variability (Antokhin et al. 1995).

Forbidden lines are useful in studies of massive stellar winds for several reasons. Foremost, they can be used to derive ion fraction abundances $\gamma_{i,E}$ (for ionization stage i of element E) from the total flux of line emission that can be used to test models of massive star evolution (Barlow et al. 1988). The lines form at very large radii in the wind, typically where the wind density is around $10^5\text{--}10^6\ \text{cm}^{-3}$ associated with the critical densities of common IR forbidden lines, and so their line profile shapes also relate directly to the geometry of the wind flow. For example, in a spherically symmetric wind, one expects a canonical “flat-topped” rectangular line profile (Castor 1970), whereas for an axisymmetric wind, the profile morphology will be double-horned or centrally peaked (Ignace & Brimeyer 2006). Moreover, at such large radii, the properties of the winds can be taken as asymptotic, and so ratios involving $\gamma_{i,E}$ for different ions within a species represent the large-scale ionization balance in the wind (e.g., Ignace et al. 2001), information that can be used to constrain the ionizing radiation field of the star.

Stellar evolution of massive stars predicts that neon should not be enriched through nuclear processing until reaching the stage of WC stars, at which point neon enrichment by factors of 10 and more are to be expected (Maeder 1983; Meynet & Maeder 2003). We show that our *Spitzer* observations generally conform to the expectation of neon enrichment. In § 2, we briefly discuss the spectra obtained with the IRS/SH instrument. In § 3, data for [Ne III] 15.56 is presented for each target, and neon abundances are derived. Conclusions based on this study are given in § 4.

2. OBSERVATIONS AND DATA REDUCTION

Target selection was based on several criteria. Sources were to be single stars and relatively bright in the infrared. We selected targets to span a range of WN and WC subtypes. All of the observations were made with *Spitzer*/IRS between February and April of 2005. The raw data were reduced using version 13.2 of the pipeline. Additional reduction involved visual inspections of each BCD frame for quality. The IRSCLEAN package was used to remove bad or hot pixels and other instrumental defects. The main reduction was conducted with the IRS tool SMART (Higdon et al. 2004). Calibration files supplied by the SMART team were used in the calibration process.

The data were cross-checked with the actual DCE FITS images to ensure that any missed bad pixels were eliminated, and that any stray instrumental effects were noted and corrected. The spectral resolving power of the IRS/SH is about 600 (Houck et al. 2004). All data were smoothed using a Gaussian with $\sigma = 0.025\ \mu\text{m}$. The method of obtaining ion fraction abundances $\gamma_{i,E}$ depends only on the total flux in the emission line, and so line profile data displayed in this paper already include subtraction of the continuum flux level at the line. As an example, Figure 1 shows part of the IRS/SH spectrum for one of our brighter sources, WR 90. The solid histogram is the smoothed IRS/SH data. The dashed line shows our fit to the continuum level. Continuum fits for all of our sources were obtained through polynomial least-squares fitting to selected line-free regions in the SH band. The continuum-subtracted data in the

TABLE 1
SUMMARY OF STAR PROPERTIES

Target	Type	d (kpc)	v_∞ (km s ⁻¹)	\dot{M} (M_\odot yr ⁻¹)	γ_e	μ_e
WR 1.....	WN4	1.8	2100	2.0×10^{-5}	1.0	4
WR 94.....	WN5	1.1	1300	2.0×10^{-5}	1.0	4
WR 75.....	WN6	4.0	2300	7.9×10^{-5}	1.0	4
WR 74.....	WN7	4.0	1300	2.5×10^{-5}	1.0	4
WR 52.....	WC4	1.5	2765	1.2×10^{-5}	0.5	3
WR 111.....	WC5	1.6	2300	0.7×10^{-5}	0.5	2.5
WR 5.....	WC6	1.9	2100	1.6×10^{-5}	0.5	3
WR 90.....	WC7	1.6	2045	2.5×10^{-5}	0.5	3

immediate vicinity of [Ne III] are displayed in Figure 2. These have not been corrected for reddening, which is quite minor at these wavelengths for our sources.

3. NEON ABUNDANCES

The line spectra are rich in He II recombination lines. The forbidden line of [Ne III] 15.56 is present and generally prominent in the spectra. Barlow et al. (1988) were the first to determine values of $\gamma_{i,E}$ from forbidden lines of WR stars, in their case for γ Vel. The principle is that forbidden lines are optically thin and form predominantly in the large radius, constant-velocity flow. Being thin, the observed total flux of forbidden line emission relates to a volume integral of the line emissivity. This integral converges and can be used to relate the ion fraction abundance $\gamma_{i,E}$ to the total line flux. Deriving ion fraction abundances does require knowledge of the wind mass-loss rate, terminal speed, and the distance to the source. Formally $\gamma_{i,E}$ sets a lower limit for the abundance of an atomic species, since the total abundance $\gamma_E =$

$\sum_i \gamma_{i,E}$. However, it is common that an element will be found in a predominant stage of ionization, with other ion stages represented in mainly trace amounts (e.g., Drew 1989). An advantage of the [Ne III] line is that one expects Ne²⁺ to be an abundant or dominant ion for many WR stars for the subtypes studied in our sample. The ionization potential (IP) for He¹⁺ is 54 eV. This is to be compared to the IP of 40 eV for Ne¹⁺, and 63 eV for Ne²⁺. At large radii helium is singly ionized (Schmutz & Hamann 1986; Hillier 1987), or even doubly ionized in many cases (W.-R. Hamann 2007, private communication). Thus, Ne²⁺ can be especially useful for tracing nuclear processing, since one reasonably expects it to represent the total abundance of neon in many instances.

The method of Barlow et al. (1988) has already been applied to a number of WR stars, for example in studies by Willis et al. (1997), Morris et al. (2000), Dessart et al. (2000), and Ignace et al. (2001) using *Infrared Space Observatory* (ISO) observations. A ground-based study by Smith & Houck (2005) determined values of γ for Ne¹⁺ for three late WN stars and a pair of late WC stars. Ion fraction abundances for EZ CMA (or WR 6, a WN4 star) based on *Spitzer* spectra have been given by Morris et al. (2004). Their models indicate that Ne²⁺ should be dominant for EZ CMA, and they find $\gamma(\text{Ne}^{2+})$ that is consistent with solar values. The general expectations of massive star evolution (Meynet & Maeder 2003) have been shown to be consistent with these observations, with neon essentially solar in WN stars and enriched in WC stars. However, the sample is still rather small, with only about 10 stars studied using the method. Our survey nearly doubles the sample.

3.1. Line Fitting Procedure

Figure 2 shows spectra for each of our stars centered on the line of [Ne III] 15.56 μm . The specific fluxes are in janskys. The filled squares are for the observed data, where blends are obvious in many cases. Forbidden lines form at large radii in the constant expansion flow and are optically thin. One thus expects flat-topped rectangular-shaped emission lines on top of the continuum. The limited resolution of the IRS leads to more rounded shapes for the lines. In Figure 2, the blend fit is shown as open circles, and the match to [Ne III] alone as the long-dashed line. For the forbidden lines, the half-widths of the profiles should represent the asymptotic wind terminal speed. Permitted lines, on the other hand, form in the vicinity of the IR pseudocontinuum (owing to the strong free-free opacity; Wright & Barlow 1975), and these lines should be narrower, since they sample the outer part of the wind acceleration that is below terminal speed. We find that the permitted lines that are blends with [Ne III] can be fit using Gaussians with $\sigma = \epsilon v_\infty$, where $\epsilon = 0.6$ has been adopted. However, Gaussians are too narrow for the forbidden lines, because the underlying profile shape is not centrally rounded like recombination lines, but intrinsically

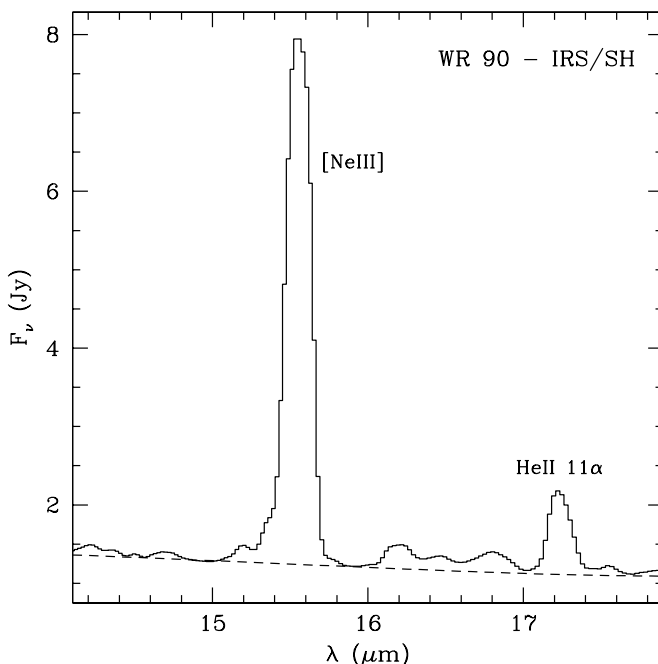


FIG. 1.— *Spitzer* IRS/SH spectra in the neighborhood of [Ne III] 15.56 μm . The line shows weak line blends on the blue side of the profile. The He II 11 α line is seen to the far right of this plot. The solid curve is the data, and the dashed curve our fit to the continuum that is subtracted from the data in order to obtain the total flux of emission in the line of [Ne III].

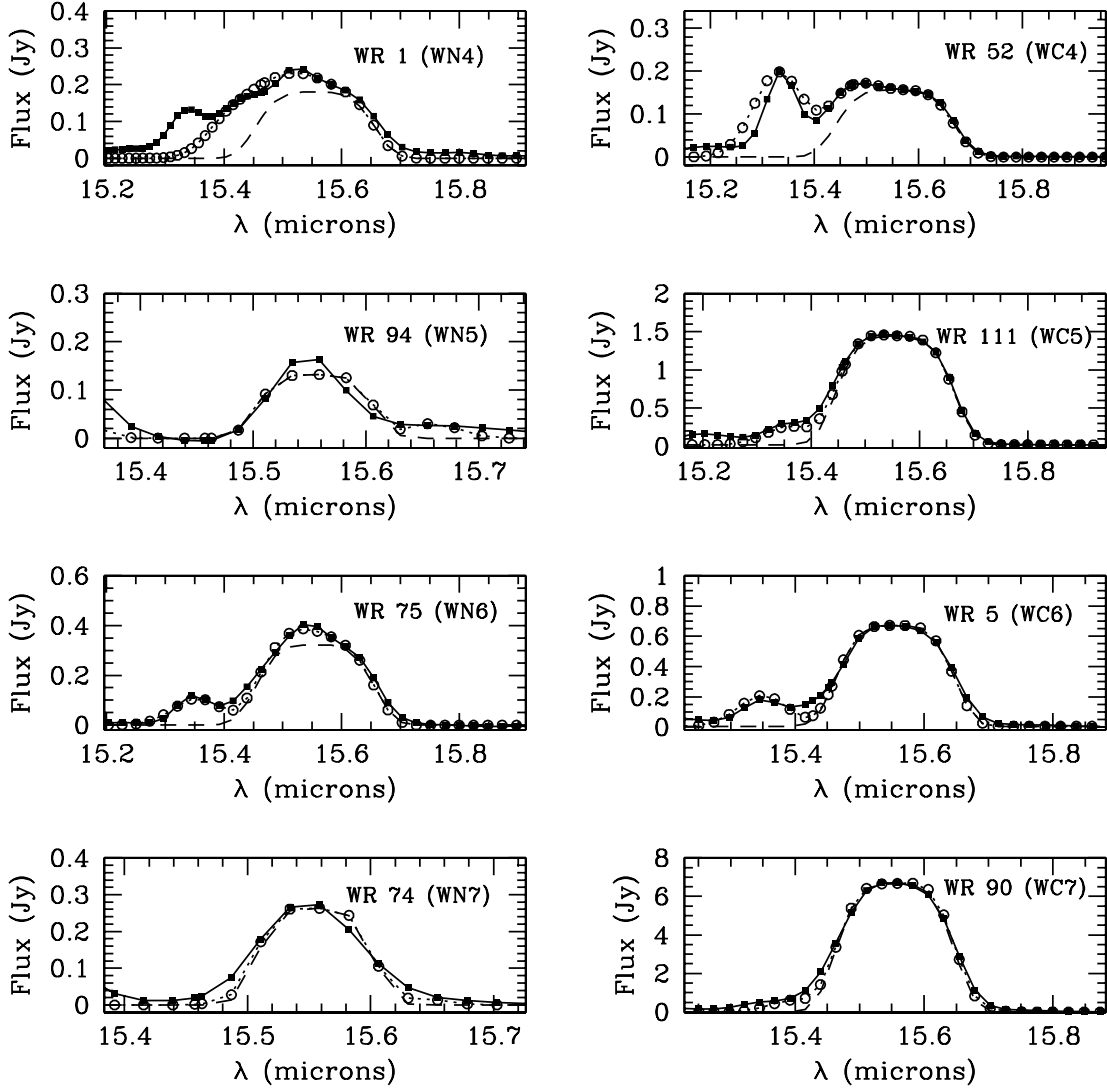


FIG. 2.—*Spitzer* IRS/SH spectra of our eight target sources centered at [Ne III] 15.56. The data are continuum subtracted, and with no dereddening applied. Filled squares are the data, open circles are fits to the lines with blends, and the long-dashed line shows the isolated fit profile for [Ne III]. Details of the profile fitting are described in the text.

rectangular, as noted above. We had to adopt a function of similar form to a Gaussian to better match the [Ne III] lines, using

$$g(\Delta v) = A_\nu \exp(-\Delta v^4/\sigma_\nu^4), \quad (1)$$

with A_ν an amplitude in janskys, Δv the observed Doppler shift in km s^{-1} , and σ_ν a line width. This function provides a symmetric profile shape that has “broader shoulders” than a Gaussian profile, required to match the broader forbidden lines, just as expected from an underlying rectangular profile shape. For example, the function $g(\Delta v)$ well approximates the shape that results from convolving a rectangular profile of half-widths appropriate for the WR winds with a Gaussian point-spread function of a width appropriate for the resolution of the IRS/SH instrument.

The HWHM for $g(\Delta v)$ is related to the wind terminal speed by $\sigma_\nu = (\ln 2)^{1/4} v_\infty \approx 0.91 v_\infty$. The total emission in the line F_l comes from integrating $g(\Delta v)$, and is analytic, as given by

$$F_l = \frac{(\ln 2)^{1/4} v_\infty}{2\lambda_0} A_\nu \Gamma(1/4), \quad (2)$$

where λ_0 is the central (vacuum) wavelength of the line, and $\Gamma(x)$ is the Gamma function. Our profile fitting allowed up to two nearby line blends along with the forbidden line. A simple algorithm was developed to step through amplitudes, and the best combination of parameters was selected through a reduced χ^2 approach.

As a rule, blends were blueward of line center, and at most only a weak feature was ever present redward of [Ne III]. Consequently, the red wing of the forbidden line was used as a gauge for selecting σ_ν . Published values of v_∞ were adopted as initial values used for σ_ν , and usually only small changes by 10% or less were needed to match the red wing.

3.2. Determination of Ion Fraction Abundances of Ne^{2+}

After obtaining fits to [Ne III] 15.56, the ion fraction abundance can be derived, with $\gamma_{i,E} = Q_i A_E$, for Q_i the ion fraction in stage i for an element E with abundance by number A_E relative to all nuclei (e.g., $A_H \approx 0.92$ for hydrogen in the Sun; Cox 2000). One has the relation $F_l = \gamma_{i,E} F_0$, where F_0 is a scale constant that depends on atomic parameters for the line transition and parameters for the stellar wind. Following the notation of Ignace & Brimeyer (2006), and correcting for the dependence on

TABLE 2
RESULTS OF LINE ANALYSES

Target	Type	$F_c(15.56 \mu\text{m})^a$ (Jy)	A_ν (Jy)	σ_v (km s ⁻¹)	D_c	F_l (erg s ⁻¹ cm ⁻²)	$\gamma(\text{Ne}^{2+})$	Ne^{2+} (Ne_\odot) ^b
WR 1.....	WN4	0.43	0.18	2300	4	4.4×10^{-13}	4.0×10^{-4}	1.1
WR 94.....	WN5	0.47	0.13	1200	4	1.7×10^{-13}	0.75×10^{-4}	0.21
WR 75.....	WN6	0.36	0.32	2300	4	7.9×10^{-13}	2.4×10^{-4}	0.67
WR 74.....	WN7	0.21	0.26	1100	4	3.1×10^{-13}	2.6×10^{-4}	0.74
WR 52.....	WC4	0.07	0.16	2600	$\approx 7^c$	4.3×10^{-13}	$10. \times 10^{-4}$	2.3
WR 111.....	WC5	0.66	1.4	2500	50	38×10^{-13}	35×10^{-4}	7.7
WR 5.....	WC6	0.23	0.67	2100	9	15×10^{-13}	15×10^{-4}	3.5
WR 90.....	WC7	1.24	6.7	2100	10	150×10^{-13}	46×10^{-4}	10.0

^a Specific flux of the continuum at 15.56 μm based on our fit to the data.

^b The solar neon abundance is the transformed value for WN (3.54×10^{-4}) or WC stars (4.48×10^{-4}), respectively, as described in the text. The adopted abundance of neon for the Sun was taken from Cox (2000). All abundances approximately double if normalizing to the value from Asplund et al. (2004).

^c This value is for the WC4 star, WR 144, inferred from Table 6 of Nugis et al. (1998).

clumping as derived by Dessart et al. (2000), the scale constant F_0 for the [Ne III] 15.56 transition is given by

$$F_0 = \frac{L_0}{4\pi d^2} = (2.27 \times 10^{-8} \text{ erg s}^{-1} \text{ cm}^{-2}) \frac{\gamma_e D_c^{1/2}}{d_{\text{kpc}}^2} \left(\frac{\dot{M}_{-5}}{\mu_e v_3} \right)^{3/2}, \quad (3)$$

where d_{kpc} is the source distance in kpc, and \dot{M}_{-5} is corrected for clumping and normalized to $10^{-5} M_\odot \text{ yr}^{-1}$, $v_3 = v_\infty / (1000 \text{ km s}^{-1})$, μ_e is the mean molecular weight per free electron, $\gamma_e = n_i/n_e$ is the number of ions per free electron, and D_c is the wind clumping factor.

One challenge to obtaining ion fraction abundances is the sensitivity of the forbidden line emission to wind clumping. Clumping has long been known to exist in WR winds and can significantly influence observables (e.g., Hillier 1991; Moffat & Robert 1994; Fullerton et al. 2006; Puls et al. 2006). To describe clumping, we adopt the clumping factor D_c as the inverse of the volume filling factor f_{cl} ; hence $D_c = f_{\text{cl}}^{-1} = \langle \rho^2 \rangle / \langle \rho \rangle^2$. Dessart et al. (2000) has shown how to correct $\gamma_{i,E}$ for the influence of clumping. The ion fraction abundance scales as $\gamma_{i,E} = F_l/F_0 \propto D_c^{-1/2} \dot{M}^{3/2}$. However, clumping factors are generally derived for the inner wind flow (e.g., Hamann & Koesterke 1998). Although there are observational and theoretical studies of how wind clumping evolves in O star winds (e.g., Runacres & Owocki 2005; Puls et al. 2006) and WR winds (e.g., Nugis et al. 1998; Hillier & Miller 1999), we do not currently know the nature of clumping in the very low density wind of 10^5 – 10^6 cm^{-3} associated with the critical densities of common forbidden lines where the line emission predominantly forms. Consequently, in future studies, new determinations of wind parameters such as clumping factors will impact the inferred values of γ presented here. In computing the value of F_0 , we adopted a collision strength of $\Omega_{12} = 1.65$ (Pradhan & Peng 1995) at an electron temperature of $T_e = 10,000 \text{ K}$ (Schmutz & Hamann 1986). In the net F_0 scales weakly with collision strength and temperature as $F_0 \propto \Omega_{12}^{1/2} T_e^{-1/4}$.

Before presenting derived values of γ for Ne^{2+} , it is necessary to discuss how these can be compared to solar abundances and model predictions. In the Sun, the abundance of neon by number is $\mathcal{A}_\odot(\text{Ne}) = 1.12 \times 10^{-4}$ (Cox 2000). During massive star evolution from O stars through the WN phase, neon is not expected to change its abundance by mass fraction; however, the relative proportion of neon nuclei by number does change, owing to the fact that hydrogen is converted to helium. In the limiting case of zero

hydrogen in WN stars, one obtains a “renormalized” unenriched neon abundance by number of

$$\mathcal{A}_{\text{WN}}(\text{Ne}) = \frac{\mathcal{A}_\odot(\text{Ne})}{0.25\mathcal{A}_\odot(\text{H}) + \mathcal{A}_\odot(\text{He})} = \frac{\mathcal{A}_\odot(\text{Ne})}{(0.25)(0.91) + 0.089} = 3.54 \times 10^{-4} \approx 3\mathcal{A}_\odot(\text{Ne}). \quad (4)$$

Renormalizing the number abundance of neon in relation to WC stars is more complicated. The ratio of C/He is changing throughout this phase, and O/He although minor, it is not entirely trivial. For reference, we ignore O and assume an equal mass fraction of He and C. Keeping the solar mass fraction of neon unchanged, the renormalized neon abundance by number becomes $\mathcal{A}_{\text{WC}}(\text{Ne}) = 4.48 \times 10^{-4} \approx 4\mathcal{A}_\odot(\text{Ne})$. Under these assumptions, the value for WC winds is not much different from WN winds, because the ratio of C/He by number is still rather low, even though the mass ratio is unity. As an upper limit, converting all of the helium to carbon would give $\mathcal{A}(\text{Ne}) = 10.6 \times 10^{-4} \approx 9\mathcal{A}_\odot(\text{Ne})$. However, in our discussion we shall adopt the value for equal mass fractions of He and C as a reference value for determining Ne enrichments.

3.3. Notes on Individual Targets

The previous section describes our technique for deriving total line fluxes from [Ne III]. The conversion of these fluxes to ion fraction abundances are described in Barlow et al. (1988) for a smooth spherical wind, and by Dessart et al. (2000) for one with constant clumping factor. Deriving $\gamma_{i,E}$ values requires knowledge of the wind terminal speed, mass-loss rate, clumping factor, and ionization/temperature state. It also requires the distance to the star be known. Stellar and wind parameters for WN stars were taken from Hamann et al. (2006). Those authors employ the Potsdam Wolf-Rayet (PoWR; Hamann & Gräfener 2004) wind models in spherical symmetry to derive wind parameters assuming a constant clumping factor of $D_c = 4$ for every star. For WC stars, parameters were taken from a variety of studies, as detailed in the description of individual objects to follow.

Distances were taken from these same papers, but in some cases we used photometric distances from the catalog of Wolf-Rayet stars by van der Hucht (2001; hereafter vdH01). It was found that distances from different sources could vary by a factor of 2 or more. Since $\gamma_{i,E}$ scales formally with the square of the distance, this is a significant concern. However, if \dot{M} is determined from radio excess measurements, then the mass-loss scales with distance as $\dot{M} \propto d^{3/2}$.

In such cases, $\gamma_{i,E} \propto d^{1/4}$, and it has a rather weak dependence on distance. Given measurement errors, uncertainties in continuum placements, line blending effects, and uncertainties in source distances, ion fraction abundances may have a factor of 2 uncertainty for our weaker sources. But even this is adequate to determine departures from solar metallicity in WC stars, since neon enrichments by factors of 10 or more are expected. The absolute flux calibration of the IRS/SH is good to only about 20% (Decin et al. 2004), which may be considered a lower limit to the uncertainty of our neon abundances, since they are determined from line fluxes.

Pertinent stellar parameters are listed in Table 1, and derived values of γ for Ne²⁺ are given in Table 2. The following sections present brief notes for selected sources. We assume that He¹⁺ is dominant in the outer winds of WN stars, and that He²⁺ is dominant for the WC stars. We also take H/He = 0 for each star.

3.3.1. WR 94 (WN5)

The ion fraction abundance of Ne²⁺ is exceptionally low for this star. The line is actually of similar strength to that observed for WR 1, and in fact the wind parameters are quite similar. The main differences are that WR 94 has about half the terminal wind speed and half the distance of WR 1. This combination leads to an ion fraction abundance around 20% solar. WR 94 shows emission at [Ne II] 12.81, but its contribution to the neon abundance is even less than Ne²⁺. We cannot explain these low values unless the wind parameters or source distance are in error

3.3.2. WR 52 (WC4)

WR 52 is the earliest of our WC types at WC4, and we have not been able to identify any tailored studies of its wind properties. It does not appear in the study of Koesterke & Hamann (1995; hereafter KH95), which in fact has no analysis for WC stars earlier than WC5. We adopt a photometric distance of 1.5 kpc from vdH01 and a wind speed of $v_\infty = 2765 \text{ km s}^{-1}$ from Prinja et al. (1990). The terminal speed is for the average of all the wind lines *except* C IV, for which Prinja et al. quote a much faster value of 3225 km s^{-1} , a value that we find much too large to match the width of the [Ne III] line.

Although KH95 have no WC4 stars from their study, Nugis & Lamers (2000) have two stars in this class. We adopt star and wind parameters based on those two stars (WR 30a and WR 144) in their Table 6. We adopt a clumping factor of $D_c = 7$ taken from WR 144 (Nugis et al. 1998). The resulting neon abundance is suspiciously low, almost solar, possibly indicating that in this early WC star, Ne³⁺ may be the dominant ion stage instead of Ne²⁺.

3.3.3. WR 111 (WC5)

We use star and wind parameters for WR 111 from the tailored analysis of Gräfener & Hamann (2005). These authors use a mass fraction of Si of 0.8×10^{-3} . With their values for He and C, we derive a Si abundance of 2×10^{-4} by number. The neon-to-silicon abundance for the Sun is 3.47 (Cox 2000). With $\gamma = 29 \times 10^{-4}$ for Ne²⁺, this implies $\text{Ne}^{2+}/\text{Si} \geq 15$. No processing of silicon is expected until very late stages of massive star evolution, so the implication is that neon is enriched by a factor of ≈ 4 , or more if some neon exists in Ne³⁺, and consistent with the value of 6.5 in Table 2. It is worth noting that using parameters derived from an independent study by Hillier & Miller (1999) yields a Ne abundance that is about 50% greater in value, due mostly to a smaller value of the volume filling factor.

3.3.4. WR 5 (WC6)

A photometric distance of 1.9 kpc is adopted from vdH01. Wind and stellar parameters are taken from KH95, except that

we lower the mass-loss rate by a factor of 3, assuming a nominal clumping factor of $D_c = 9$.

3.3.5. WR 90 (WC7)

The star with our latest WC type is WR 90, at WC7. Stellar parameters from Dessart et al. (2000) are adopted. Those authors obtained *ISO* data of a similar spectral range as our *Spitzer* data. They measured $F_l = 6.5 \times 10^{-12} \text{ erg s}^{-1} \text{ cm}^{-2}$ from [Ne III] 15.56. Our derived value is a little more than twice the value of that paper. However, the data of Dessart et al. are quite noisy, and without knowing how their data were processed or where their continuum level was placed, it is difficult to determine the cause of this difference.

4. CONCLUSIONS

Our survey approximately doubles the sample of neon abundances derived for Galactic WC stars, and substantially increases the number of such instances at spectral subtypes of high ionization (earlier than WC8). Our analysis of [Ne III] 15.56 μm of four WN stars and four WC stars appear to be generally consistent with the expectations of massive star evolution theory (Maeder 1983; Meynet & Maeder 2003): (1) The ion fraction abundances of Ne²⁺ are consistent with solar proportions of neon in the WN stars, as expected, and (2) those for the WC stars show enhanced values of Ne²⁺. Formally, our derived values are lower limits to the neon abundances in the sense that neon can exist in more than one ion stage. At large radii where the forbidden line forms, He¹⁺ or He²⁺ will be dominant, and a consideration of ionization potentials suggests that Ne²⁺ will probably be the dominant ion for many WR winds. Our survey does not include lower ionization WR stars, such as the WN8-10 and WC8-9 stars, where Ne¹⁺ is more likely to be a significant ion stage of neon (cf. the discussion of Smith & Houck 2005). However, uncertainties in distance, deblending, continuum placement, and clumping factors may allow for a factor of 2 uncertainty in derived ion fraction abundances of Ne²⁺ in some of our weaker sources.

It is worth commenting that our understanding of wind clumping and its distribution throughout hot star winds is still somewhat poor. As a limit, should clumping disappear altogether in the very low density outer wind (e.g., Puls et al. [2006] find empirically that clumping decreases with radius in O star winds), all of the values of $\gamma(\text{Ne}^{2+})$ would double for the WN stars (and still remain largely solar), but triple or more for the WC stars. On the other hand, if the winds become increasingly clumped, our γ values would need to be revised downward. Taking straight averages, the ratio of Ne²⁺ for the four WC stars as compared to that of the four WN stars is almost a factor of 9.

As one final note, in drawing conclusions about neon abundances for our sources, we have adopted solar abundances from Cox (2000). Morris et al. (2004) and Smith & Houck (2005) both reference the Asplund et al. (2004) value of solar neon that is 1.8 times smaller than Cox (2000). Such a value would nearly double the neon enrichments inferred for the stars of our sample. It is clear that future progress in the quantitative assessment of massive star evolution theory against observational data will require several things: better distances to WR stars, better knowledge of wind clumping factors, and a resolution to the appropriate neon abundance for use as a reference point of chemical enrichments.

We are appreciative of several helpful comments made by an anonymous referee. We gratefully acknowledge funding support from NASA grants RSA-1264363, RSA-1265387, and RSA-1265401.

REFERENCES

- Antokhin, I., Bertrand, J.-F., Lamontagne, R., Moffat, A. F. J., & Matthews, J. 1995, *AJ*, 109, 817
- Asplund, M., Grevesse, N., Sauval, A. J., Allende Prieto, C., & Kiselman, D. 2004, *A&A*, 417, 751
- Barlow, M. J., Roche, P. F., & Aitken, D. K. 1988, *MNRAS*, 232, 821
- Castor, J. I. 1970, *MNRAS*, 149, 111
- Cox, A. N., ed. 2000, *Allen's Astrophysical Quantities* (4th ed.; New York: AIP)
- Decin, L., Morris, P. W., Appleton, P. N., Charmandaris, V., Armus, L., & Houck, J. R. 2004, *ApJS*, 154, 408
- Dessart, L., Crowther, P. A., Hillier, D. J., Willis, A. J., Morris, P. W., & van der Hucht, K. A. 2000, *MNRAS*, 315, 407
- Drew, J. E. 1989, *ApJS*, 71, 267
- Fullerton, A. W., Massa, D. L., & Prinja, R. K. 2006, *ApJ*, 637, 1025
- Gräfener, G., & Hamann, W.-R. 2005, *A&A*, 432, 633
- Hamann, W.-R., & Gräfener, G. 2004, *A&A*, 427, 697
- Hamann, W.-R., Gräfener, G., & Liermann, A. 2006, *A&A*, 457, 1015
- Hamann, W.-R., & Koesterke, L. 1998, *A&A*, 335, 1003
- Higdon, S. J. U., Devost, D., Higdon, J. L., Brandl, B. R., Houck, J. R., et al., 2004, *PASP*, 116, 975
- Hillier, D. J. 1987, *ApJS*, 63, 947
- . 1991, *A&A*, 247, 455
- Hillier, D. J., & Miller, D. L. 1999, *ApJ*, 519, 354
- Houck, J. R., Roellig, T. L., van Cleve, J., Forrest, W. J., Herter, T., Lawrence, C. R., et al., 2004, *ApJS*, 154, 18
- Ignace, R., & Brimeyer, A. 2006, *MNRAS*, 371, 343
- Ignace, R., Cassinelli, Quigley, M., & Babler, B. 2001, *ApJ*, 558, 771
- Koesterke, L., & Hamann, W.-R. 1995, *A&A*, 299, 503 (KH95)
- Lamers, H. J. G. L. M., Maeder, A., Schmutz, W., & Cassinelli, J. P. 1991, *ApJ*, 368, 538
- Maeder, A. 1983, *A&A*, 120, 113
- Meynet, G., & Maeder, A. 2003, *A&A*, 404, 975
- Moffat, A. F. J., & Robert, C. 1994, *ApJ*, 421, 310
- Monnier, J. D., Tuthill, P. G., Danchi, W. C., Murphy, N., & Harries, T. J. 2007, *ApJ*, 655, 1033
- Morris, P. W., Crowther, P. A., & Houck, J. R. 2004, *ApJS*, 154, 413
- Morris, P. W., van der Hucht, K. A., Crowther, P. A., Hillier, D. J., Dessart, L., Williams, P. M., et al., 2000, *A&A*, 353, 624
- Nugis, T., Crowther, P. A., & Willis, A. J. 1998, *A&A*, 333, 956
- Nugis, T., & Lamers, H. J. G. L. M. 2000, *A&A*, 360, 227
- Pradhan, A. K., & Peng, J. 1995, in *Space Telescope Science Inst. Symp. Ser. 8, The Analysis of Emission Lines*, ed. R. E. Williams & M. Livio (Cambridge: Cambridge Univ. Press), 8
- Prinja, R. K., Barlow, M. J., & Howarth, I. D. 1990, *ApJ*, 361, 607
- Puls, J., Markova, N., Scuderi, S., Stanghellini, C., Taranova, O. G., Burnley, A. W., et al., 2006, *A&A*, 454, 625
- Runacres, M. C., & Owocki, S. P. 2005, *A&A*, 429, 323
- Schmutz, W., & Hamann, W.-R. 1986, *A&A*, 166, L11
- Smith, J.-D. T., & Houck, J. R. 2005, *ApJ*, 622, 1044
- van der Hucht, K. A. 2001, *NewA Rev.*, 45, 135 (vdH01)
- van der Hucht, K. A., Conti, P. S., Lundström, I., & Stenholm, B. 1981, *Space Sci. Rev.*, 28, 227
- Williams, P. M. 1997, *Ap&SS*, 251, 321
- Willis, A. J., Dessart, L., Crowther, P. A., Morris, P. W., Maeder, A., Conti, P. S., et al., 1997, *MNRAS*, 290, 371
- Wright, A. E., & Barlow, M. J. 1975, *MNRAS*, 170, 41